Geotextiles and Geomembranes 49 (2021) 910–920

Contents lists available at ScienceDirect

Geotextiles and Geomembranes

journal homepage: www.elsevier.com/locate/geotexmem

Shear strength characteristics of geosynthetic reinforced rubber-sand mixtures

D.R. Manohar, P. Anbazhagan [1,*]

Department of Civil Engineering, Nagarjuna College of Engineering and Technology, Bangalore, India

ARTICLE INFO

Keywords:
Geosynthetics
Brittleness index
Energy absorption
Triaxial test
Shear strength

ABSTRACT

Shear strength characteristics of the geosynthetic-reinforced rubber-sand mixture (RSM) has been investigated by conducting Unconsolidated Undrained (UU) triaxial test. In the first part, a series of UU triaxial tests have been carried out to know the size effect of granulated rubber/tyre chips from seven different rubber sizes. RSM sample that provides higher strength, energy absorption capacity and stiffness is considered as the optimal size and has been used in the investigation on geosynthetic-reinforced RSM. In the second part, shear strength characteristics of geosynthetic-reinforced RSM has been investigated by varying proportions of rubber content (50% and 75% rubber by volume), type of geosynthetic (geotextile, geogrid and geonets), number of geosynthetics (1–4) layers, geosynthetic arrangement and confining pressure. The results demonstrate that RSM reinforced with geosynthetic has enhanced peak strength, failure strength and corresponding axial strain at failure. Fifty percent RSM reinforced by geotextile and 75% RSM reinforced by geonets with 4 layers of reinforcement, led to a maximum increase in shear strength. The strength and energy absorption capacity are doubled for the reinforced RSM's, and reduced the brittleness index values as close to zero, which depends on the type, number of layers and arrangement of geosynthetic.

1. Introduction

Natural and man-made vibrations are undesirable for structures, as structural stability, durability, and performance are affected considerably. Vibrations which are transmitted through the ground can cause excessive stresses in the structures, resulting in a collapse of structures accompanied by disastrous physical and economic consequences (Hazarika et al., 2008; Kirzhner et al., 2006). Backmann and Ammann (1987) have proposed the limits on allowed levels of vibrations tolerated by structures and machines from different regulations. Vibration reduction can be attained either by increasing the damping capacity or by increasing stiffness of the structure and the construction materials. Rubber is commonly used as a vibration-damping material due to its viscoelasticity (Ganeriwala, 1995; Tsang, 2008; Tsang et al., 2012). The damping properties of the granulated rubber/tyre chips derived from the waste tyres are yet to be exploited to use them effectively in common civil engineering applications. Scrap tyre derived recycled products (such as granulated rubber, tyre chips and tyre shreds) has been called "smart-geomaterial," due to their good permeability, high strength, compressibility, and the absence of strain localization (Hazarika et al., 2008a; Sheikh et al., 2013).

One promising approach in waste tyre utilization is vibration reduction and seismic isolation of building taking into account the high damping behaviour in rubber (Hazarika, 2008; Hazarika et al., 2008b; Senetakis et al., 2012; Tsang, 2008; Tsang et al., 2012). However, systematic studies of using RSM as vibration isolation materials are limited. Anbazhagan et al. (2017) concluded that parameters influencing shear strength and compressibility characteristics of RSM were rubber size, unit weight of RSM, rubber content, aspect ratio and confining pressure. Waste tyres are mixed with sand and used in geotechnical applications in order to overcome the potential problem such as spontaneous combustion and compressibility (Bosscher et al., 1997). Bosscher et al. (1997) reported that the compressibility of tyre chips could be reduced significantly by adding 30–40% sand by volume. For higher rubber content in RSM, shear strength of RSM reduces when compared to soil. In order to overcome this, geosynthetic is placed within RSM to increase vertical confinement of the system. The main role of reinforcement is to improve the engineering properties of soil. Geogrid and geotextile have been

* Corresponding author. Department of Civil Engineering, Indian Institute of Science, Bangalore, 560 012, India.
E-mail addresses: anbazhagan@iisc.ac.in, anbazhagan2005@gmail.com (P. Anbazhagan).
[1] http://civil.iisc.ernet.in/~anbazhagan/.

https://doi.org/10.1016/j.geotexmem.2020.12.015
Received 4 March 2020; Received in revised form 31 December 2020; Accepted 31 December 2020
Available online 21 January 2021

widely used in earthworks to improve Strength characteristics of soil (Chawla et al., 2019; Javad et al., 2020). Laboratory studies and numerical simulations have been carried out to investigate the bearing capacity, deformation characteristics and failure mechanism of geosynthetic-reinforced soil structures (Satyal et al., 2018; Shadmand et al., 2018; Dash and Choudhary, 2018; Song et al., 2018; Dehkordi et al., 2019; Tafreshi et al., 2019, 2020; Ghotbi Siabila et al., 2020; Fei et al., 2020).

This study investigates the effect of geosynthetic reinforcement on the shear strength characteristics and energy absorption capacity of RSM through triaxial compression test. Three types of geosynthetics (geogrid, geonets and geotextile) were used for reinforcing RSM in layered form. Different kinds of geosynthetics were used because different types have different stress-deformation characteristics (Junyi Duan et al., 2021; Mehrjardi et al., 2019). Parameters such as depth of geogrid/geocells, the spacing between the geogrid layers and number of geogrid layers influence bearing capacity and settlement characteristics of reinforced soil (Selcuk and Mustafa, 2020; Han et al., 2019; Correia and Zornberg, 2018; Wang et al., 2018; Venkateswarlu et al., 2018; Mousavi et al., 2017). Using geosynthetics as reinforcing materials increases shear strength through friction and has an added advantage of increased ductility. Geosynthetic-reinforced soil showed higher ultimate bearing capacity and better settlement control and differential settlement than unreinforced soil (Liang et al., 2021; Muhammad et al., 2020). Another advantage is that reinforcement provides a liquefaction resistance under cyclic loading and a smaller loss of post-peak shear strength compared to unreinforced soil (Soheil Ghadr et al., 2020).

A series of UU triaxial tests have been carried out to select the optimum size of rubber for the reinforcement study, from seven different rubber sizes. The rubber size that provides comparatively higher shear strength, ductility and stiffness is considered as the optimal size and has been further used in the investigation on geosynthetic-reinforced RSM. The mechanical behaviour of geosynthetic-reinforced RSM has been investigated by varying proportions of rubber (50% and 75%), type of geosynthetic (geotextile, geogrid and geonets), number of geosynthetic layers (1–4 layers), geosynthetic arrangement and confining pressure (20, 60 and 100 kPa). The results are analyzed to select the suitable type of reinforcement, which gives higher shear strength without affecting damping characteristics of the selected composition of RSM.

2. Background

Much research was carried out to understand the beneficial effects of tyre derived aggregate as lightweight fill for embankments and retaining walls (Bergado et al., 2008; Edincliler, 2008; Edincliler et al., 2010; Humphery, 2008; Masad et al., 1996; Lee et al., 1999). Several studies are also available on the use of rubber/rubber sand mixtures as a novel application for seismic disaster mitigation for retaining wall and waterfront structures (Hazarika, 2008; Hazarika et al., 2008b). Some onsite experimental studies are also available for isolation of ground vibration using pressed scrap tyres (Hayakawa et al., 2008). Tatlisoz et al. (1998) evaluated the mechanical properties of soil-tyre chip mixtures relevant to geosynthetic-reinforced earthworks, for the potential advantage of using soil-tyre chips backfills for retaining walls and embankments. Tsang (2009) mentioned the seismic isolation system involving RSM, which involves the concepts of geotechnics as Geotechnical Seismic Isolation, in contrast to the commonly used structural seismic isolation. Tsang (2009) also discussed the ideas of utilizing geosynthetics as base isolation system proposed by Yegian and Kadakal (2004) and Yegian and Catan (2004). Two different approaches were adopted to use geosynthetic as base isolation. Geosynthetic liners were placed underneath the foundation of a structure and placed within the soil at some depth below the foundations so as to prevent seismic energy. Yoon et al. (2008) and Yoon (2008), used waste tyre as reinforcing material by eliminating sidewalls to make tyre mat, tread-mat, and three-dimensional cell type tyres to reinforce sand. Some numerical studies were carried out by using RSM (50–75% rubber by volume in RSM) as replacement of soils to mitigate earthquake induced ground motions (Anastasiadis et al., 2012; Kaneko et al., 2013; Xiong et al., 2014; Pitilakis et al., 2015; Santiago et al., 2016; Tsang, 2008; Tsang et al., 2012). The numerical studies didn't consider high compressibility of RSM as it may lead to higher settlement levels in comparison to conventional soil layers. In addition, minimal studies are carried out for reinforcing composite materials such as RSM using geosynthetic reinforcement, to enhance the load-carrying capacity without affecting the damping characteristics.

On the other side, scrap tyres are generated one per capita annually in many of the countries (Edil and Bosscher, 1994), in particular developing countries facing significant disposal problem. Increasing of the industry and a growing population has resulted in hundreds of millions of scrap tyres, which are disposed of around the world every year. It is increasingly becoming harder and expensive to dispose of them safely without any threat to human health and the environment. This situation has produced a need to find new beneficial ways of recycling waste tyres. One approach consists of shredding the tyres into small pieces that are often referred to as tyre chips, tyre shreds or tyre crumbs, depending on their size. The use of shredded tyres alone or mixed with sand (RSM) can be used to replace aggregate, improve drainage, and provide thermal insulation (Benson et al., 1996; Edil and Bosscher, 1994; Humphery, 2008). Over the last few years, recycling of waste materials as construction materials has been considered essential to solve economical and technical problems for a sustainable environment. Though current reuse and recovery efforts have slightly reduced the number of landfills, still there is a need to develop an additional practice for the reuse of scrap tyres. Utilizing rubber tyres in vibration mitigation due to its high energy absorption capacity can be a viable approach to resolve chronic problems associated with the disposal of waste tyres.

3. Need for the study

Composites of raw materials in tyre have unique properties such as flexibility, strength, resiliency, and high frictional resistance. Above properties are altered after use in the vehicle (i.e. scraped tyres), however a considerable amount of above properties still remains in the waste tyres. Exploiting the inherent properties of scrap tyres not only helps in effective disposal of waste tyres but also solves some technical problems in geotechnical engineering. By exploring the above unique properties, Tsang (2008); Tsang et al. (2012) proposed the seismic isolation system for low-to-medium rise buildings using RSM's through numerical studies. The method involves mixing shredded rubber tyre particles with soil (75% rubber and 25% sand) and placing the mixtures around building foundations, which provides a function similar to that of the cushion. Tsang et al. (2012) developed a finite element program for modeling the dynamic response of the soil-foundation-structure system and evaluated the effectiveness of their proposed method. Authors concluded that the structural response in terms of horizontal acceleration at each floor and inter-storey drift could be reduced by 40–60%. Pitilakis et al. (2015) investigated the seismic response of reinforced concrete buildings on soil replaced with rubber-sand mixtures. Dynamic analyses of the soil-structure systems were performed for the variation of RSM layer thickness, building height and different input motions. The numerical study suggested that, reduction in base shear and maximum interstorey drift up to 40% and 30% in comparison to the soil profile. Santiago et al. (2016) carried out a non-linear analysis to check the effectiveness of seismic isolation system composed of sand and shredded rubber mix. Analyses were carried out by varying layers of RSM and input accelerations and concluded that 2–3 m of a shallow layer of RSM is enough to achieve reductions in the seismic response of structures. Anbazhagan et al. (2015), also investigated the effectiveness of the proposed isolation technique, using rubber-soil mixtures through numerical simulations (Refer, Fig. 1). The response of structures in terms of

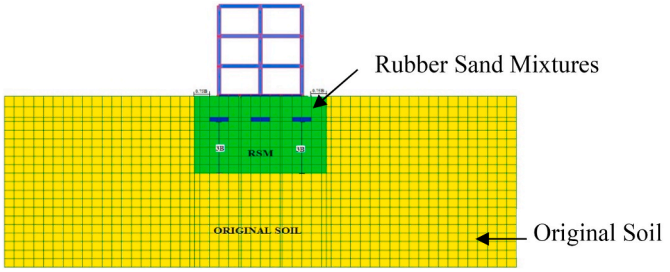

Fig. 1. Finite element model for the proposed seismic isolation method using RSM layer (Anbazhagan et al., 2015).

acceleration and inter-storey drift at different floor levels was recorded and found that acceleration at different floor level was reduced by 40–50%. Fig. 1 shows the configuration of the system involving seismic isolation using RSM. This study intends to solve the problems of strength and deformability of RSM as foundation materials by reinforcing RSM with geosynthetics. From the numerical studies on RSM as vibration isolation material, it suggests that higher the rubber content in RSM, higher will be the viscoelasticity of the RSM, and higher will be the effectiveness of the proposed scheme. Zornberg et al. (2004) have reported that for the rubber content of 60% by volume and above, rubber-soil mixture's exhibit low shear strength and high compressibility.

It can be noted from the previous studies that, higher rubber content in RSM (up to 75% rubber and 25% sand) showed lower strength and higher damping than pure soil. Thus, high damping composite materials such as RSM have proven to be suitable for vibration isolation. However, high compressibility of RSM's constitutes a disadvantage of the mixtures as it may lead to higher settlement levels compared to conventional soil layers. With higher rubber content, the behaviour of RSM changes from composite material like behaviour to rubber-like behaviour. Thus with the further increase in rubber content beyond 75%, RSM behaves like rubber materials with higher compressibility (Moghaddas Tafreshi and Norouzi, 2012; Pitilakis et al., 2015). In order to enhance the load carrying capacity of RSM, the geosynthetic-reinforcement study has been carried out considering 50% and 75% rubber by volume in RSM. Prior to the reinforcement study, UU triaxial tests were carried out to know the influence of rubber size on shear strength characteristics and energy absorption capacity of RSM similar to Anbazhagan et al. (2017). Anbazhagan et al. (2017) highlighted that many studies carried out to find the shear strength of RSM was conducted by considering one particular size of rubber or varying sizes of tyre shreds/chips. To know the influence of rubber size and composition on strength characteristics of RSM, seven different rubber sizes were selected. The rubber size, which gives higher shear strength and energy absorption capacity compared to other rubber sizes, is considered as optimum size and further used for reinforcement study.

4. Materials used

4.1. Sand

In the present study, the locally available sand was used. The soil particles used in the present study were granular in nature, passing through a 4.75 mm sieve. The primary properties such as grain size distribution, maximum and minimum dry density, specific gravity, coefficient of curvature and uniformity coefficient of sand were determined. The grain size of sand varied between 0.075 mm and 4.75 mm, and its distribution curve is shown in Fig. 2a. The specific gravity of the sand is 2.65, estimated as per ASTM D854 (2010). The sand is classified as uniformly graded sand according to the unified classification system (UCS), ASTM-D2487 (2003). Other details of sand are presented in Table 1.

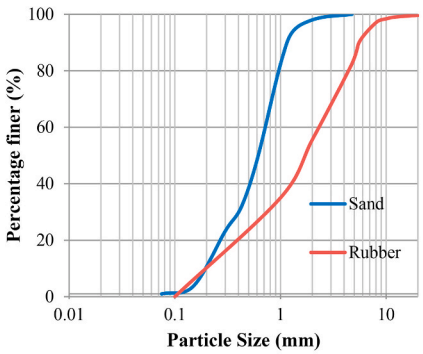

2 (a)

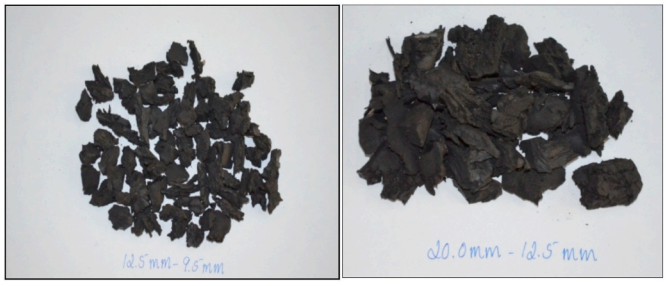

2 (b)

Fig. 2. (a) Particle size distribution curve of sand and rubber (b) Typical rubber sample for rubber size E and G.

Table 1
Properties of sand.

Description	Value
Effective size, D_{10}	0.2 mm
D_{30}	0.4 mm
Mean size, D_{50}	0.6 mm
D_{60}	0.71 mm
Uniformity coefficient (Cu)	3.55
Curvature coefficient (Cc)	1.13
Specific Gravity	2.65
Maximum dry density	1.786 g/cm^3
Minimum dry density	1.434 g/cm^3
Relative density adopted	80%
Friction angle	35°

4.2. Rubber

The waste tyre crushed rubber was procured from the local industry; Vaibhav Rubbers (Thane, Maharashtra, India), which were prepared with special machinery by removing the steel belting from scrap tyres then crushing into pieces and powder. The procured rubber grains were angular and had rough sides. As per ASTM D6270 (2008), particulate rubber composed of non-spherical particles with size ranges from 425 μm to 12 mm is referred to as granulated rubber. Scrap tyre pieces between 12 mm and 50 mm are referred to as tyre chips. These were sieved and separated into groups (A to G) as per particle sizes, and its distribution curve is shown in Fig. 2a. In the present study, rubbers are grouped into different groups based on particle size, group A (passing 2 mm sieve and retained on 1 mm sieve), group B (4.75 mm–2 mm), group C (5.6 mm–4.75 mm), group D (8 mm–5.6 mm), group E (9.5 mm–8 mm), group F (12.5 mm–9.5 mm) and group G (20 mm–12.5 mm). Of

these, six groups (A to F) can be called as granulated rubber and group G, is called as tyre chips (ASTM D6270, 2008). Typical photos of rubber samples of rubber size E and G is shown in Fig. 2b. The water absorption of rubber (in percentage) was found to be 3.84 (A), 3.86 (B), 3.83 (C), 3.85 (D), 3.86 (E), 3.87 (F) and 3.85 (G). The average value of water absorption of rubber is 3.85, according to ASTM-C128 (2007a). The specific gravity of rubber grains for A, B, C, D, E, F and G were found to be 1.11, 1.13, 1.14, 1.14, 1.16, 1.17 and 1.16 respectively, based on ASTM-D854 (2010) procedures. The average value of the specific gravity of considered rubber sizes was found to be 1.14. Similarly, the maximum densities of granulated rubber/tyre chips as per above-quoted respective sizes were 4.7, 5.4, 6.2, 6.45, 6.71, 6.9 and 6.6 kN/m^3. The applications where shredded rubber alone or shredded rubber-soil mixtures are utilized as construction materials, special recommendations should be followed during the design and construction stage according to ASTM D6270 (2008).

4.3. Geo-synthetics

Three types of geosynthetics have been selected for reinforcement, namely geotextile, geonets and geogrids. The physical and mechanical properties of geo-synthetics are presented in Table 2. The load elongation behaviour of the geosynthetics in the wide width tension test is determined according to ASTM D6637 (2011), and the load elongation behaviour is shown in Fig. 3a. Types of geo-synthetics used in the present study are shown in Fig. 3b.

5. Experimental program

To investigate the effects of rubber size on shear strength and energy absorption capacity of RSM, a total of 130 Unconsolidated Undrained (UU) triaxial compression tests were performed. The test parameters considered in this study were rubber size (A to G), rubber content (10–35%) and confining pressure (20, 60 and 100 kPa). Based on these test results, rubber size, which gives higher shear strength compared to other rubber size is considered as optimum size and further used for geosynthetic reinforcement study. In the second part of this study, to study the effects of various parameters on the mechanical behaviour of geosynthetic reinforced RSM, a total of 132 UU triaxial tests are performed. The test parameters include; the percentage of rubber content (50% and 75%), type of geosynthetic (geogrid, geonet, and geotextile), number of geosynthetic layers (1–4 layers), geosynthetic arrangements as shown in Fig. 4 and confining pressure (20, 60 and 100 kPa).

5.1. Sample preparation and testing procedure

The amount of sand and rubber required for each percentage composition was estimated for all the granulated rubber sizes. RSM has been prepared for 10%, 15%, 20%, 25%, 30%, 35%, 50% and 75% rubber by volume (volume of the rubber/total volume of the specimen). The corresponding volume of sand for above mentioned rubber percentages are 90%, 85%, 80%, 75%, 70%, 65%, 50% and 25% sand by volume. Rubber was mixed with sand on a volumetric basis because volumetric specification would be easier to implement in the field. However, sample preparation in the laboratory was performed using the measurement of weight instead of volume. Thus, the volume has been calculated by known weight and specific gravity. Sand-Rubber

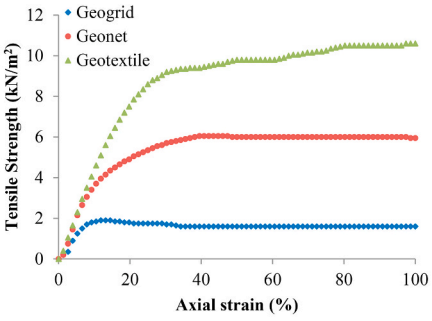

3 (a)

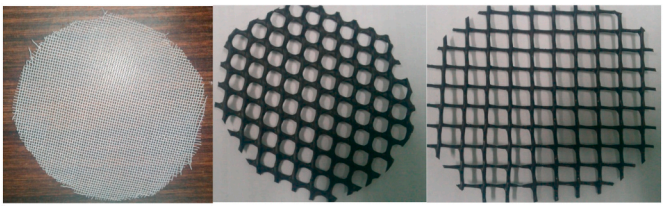

Geotextile *Geonet* *Geogrid*

3 (b)

Fig. 3. (a) Load elongation behaviour of geosynthetics, (b) Types of geo-synthetics used in present study.

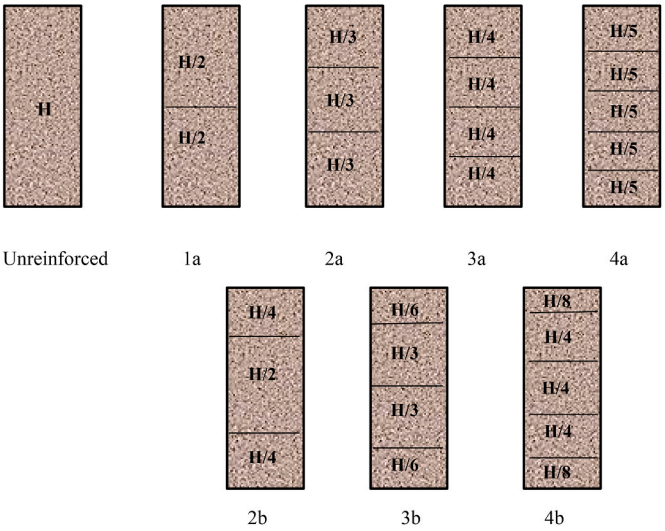

Fig. 4. Geosynthetic arrangements for triaxial tests (H: height of the sample).

Table 2
Mechanical properties of geosynthetic material.

Type of geo-synthetic material	Mass (g/m^2)	Thickness (mm)	Effective opening size (mm)	Ultimate tensile strength (kN/m^2)	Axial strain at failure (%)	Secant modulus at 5% strain
Geogrid	39.2	1.0	9.0	1.60	14.47	40
Geonet	74.4	1.5	8.0	5.95	47.37	50
Geotextile	21.4	0.3	1.0	9.50	107.89	60

specimens were prepared by hand mixing with dry sand. The RSM's were transferred into the mould in layers with uniform mixing to avoid segregation during the sample preparation. The prepared RSM samples were poured into vacuum split mould in 4–5 layers to achieve a uniform mix and were slightly compacted for a higher percentage of rubber. The UU triaxial tests were carried out on sample size of 50 × 100 mm for rubber sizes A to D, and 100 × 200 mm for rubber size of E to G for the respective samples of RSM, at a relative density of 80% (refer Fig. 5) and for effective confining pressures of 20, 60 and 100 kPa to select the optimum size of rubber. After the application of confining pressure to the RSM samples, approximately 10–15 min was allowed to stabilize, before shearing. The samples were tested according to ASTM D-2850, (2007b), and tests were carried out on RSM at a constant strain rate of 1.25 mm/min.

All reinforcement tests were conducted with a sample size of 100 × 200 mm with geosynthetics arranged in horizontal layers where each layer was arranged with equal space ratio and varying space ratio, as shown in Fig. 4. The test specimens are prepared by a procedure similar to that adopted for UU test on RSM. Geosynthetics were arranged in horizontal layers, as this could improve the strength mainly by friction, and interlocking between soil and the reinforcement. The diameter of the reinforcement was slightly less than that of the sample. UU triaxial tests on geosynthetic reinforced RSM were carried out on a sample size of 100 × 200 mm, at the strain rate of 1.25 mm/min.

6. Results and discussion

The strength characteristics and energy absorption capacity of the RSM were examined through UU triaxial test in order to know the influence of rubber size by selecting different size range (A to G). To enhance the shear properties of compressible RSM, reinforcement study was carried out. The results of the geosynthetic reinforcement with RSM through laboratory tests are presented in the second part of this study, with a discussion highlighting the effects of various parameters.

6.1. Stress-strain behaviour and rubber size effect

Typical trends of stress-strain curves obtained from UU triaxial tests for confining pressure of 100 kPa for granulated rubber size F with different percentage of rubber are shown in Fig. 6. The influence of rubber content could be noticed by the significant change in the stress-strain behaviour. The addition of rubber to sand increases the initial slope of the stress-strain curve, which indicates RSM will have more strength at small strain values. The deviatoric stress increases with an increase in the rubber content up to 30%, with no further increase thereafter. But the value of deviatoric stress at all percentages is found to be greater than the deviatoric stress for sand. However, the axial strain corresponding to peak deviatoric stress increases with the increasing rubber content. The axial strain at failure was also found to increase, especially at a higher percentage of rubber (i.e. 35 % rubber by volume in RSM). Peak strength, ultimate strength, corresponding axial strain, and ductility were enhanced with increasing rubber content. Adding

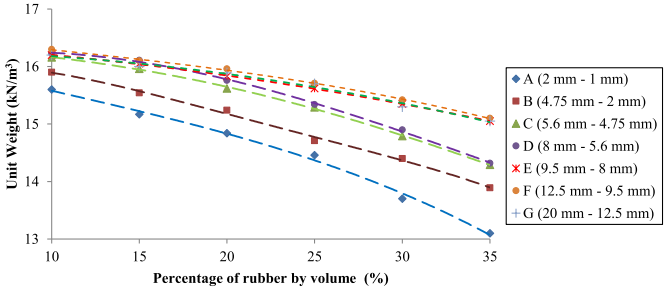

Fig. 5. Unit weight plot for different rubber sizes and rubber content.

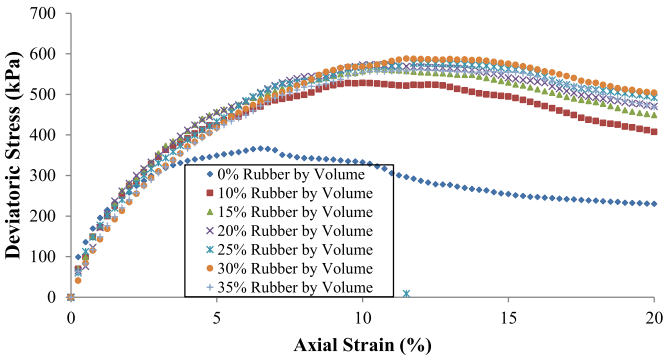

Fig. 6. Stress-Strain Curve for rubber size F, for confining pressure of 100 kPa with different composition of rubber in RSM.

10–30% of rubber to sand particles enhances the shear strength in comparison to clean sand, which may be because of two reasons. First, the sand can accommodate more particles of rubber sizes A and B due to similar grain sizes. The voids created by rubber grains are occupied by the sand for rubber sizes A and B, and for other rubber sizes (C–G) rubber particles act as reinforcement for the sand. With the increase in the length of rubber, the shear strength of RSM increases up to rubber size F, thereafter it starts decreasing for larger rubber size G. This decrease in strength might be due to decrease in the unit weight of RSM for rubber size G than F. Thus, compared to clean sand, the strength of RSM is enhanced. Second, the addition of more rubber results in creating more voids in RSM, which starts adversely affecting its strength. The decrease in peak stress observed at higher rubber content (35% rubber by volume) is due to increase in the quantity of rubber in failure plane and the rubber–rubber particle friction will have a larger influence. This behaviour is observed in almost all rubber sizes.

The optimum percentage mix of rubber for enhanced shear strength of RSM varies for different sizes of rubber (A to G). From overall observation, it was noted that, for rubber size A and B, 20% rubber by volume was found to be optimum, 25% rubber by volume was found to be optimum for rubber size C and D, and for rubber size E, F and G, 30% rubber by volume was determined to be optimum, giving the maximum shear strength. In this study, the shear properties of sand were increased with the addition of rubber, which might be due to the influence of rubber length, aspect ratio (length/diameter), stiffness of rubber particles, the orientation of rubber, sand friction angle and confining stress.

6.1.1. Energy absorption capacity and ductility

The unique advantage of scrap tyre when compared to any other waste materials is the improvement of ductility and energy absorption capacity as a composite engineering material. The area under the stress-strain curve up to a given value of strain is the total mechanical energy per unit volume consumed by the material while straining it to that value (Roylance, 2001). This is given by,

$$EA = \int_0^{\in} \sigma(\in)\, d\in$$

where $\sigma(\in)$ is the stress as a function of the strain. The measure of ductility is given by the brittleness index, which is a function of failure and ultimate deviatoric stress. The measure of this behaviour can be given by the brittleness index (I_B),

$$I_B = \frac{q_f}{q_{ult}} - 1$$

where, q_f and q_{ult} are the failure and the ultimate deviatoric stresses. The complete details about how to calculate, energy absorption capacity and ductility of RSM can be referred in Anbazhagan and Manohar (2015). A typical plot of energy absorption capacity for different rubber sizes (A to

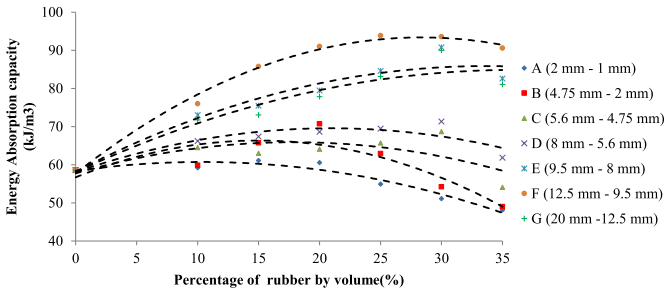

Fig. 7. Typical plot of energy absorption capacity for different rubber sizes and contents for confining pressure of 100 kPa.

G) and composition for confining pressure of 100 kPa is shown in Fig. 7, by tracing out the area under stress-strain curve up to an axial strain of 20%. It is shown that the energy absorption capacity increases with the increasing rubber content, which is due to the increase in peak and ultimate stresses. The same trend could be observed in the composite for all sizes of rubber, and it increases with increasing rubber size up to rubber size F thereafter it decreases (i.e., rubber size G). Similarly, the typical plot of brittleness index for different rubber sizes (A to G) and composition for confining pressure of 100 kPa is shown in Fig. 8. This study indicates that brittleness index of sand decreases with the increasing percentage of rubber up to a certain extent for different rubber sizes, thereafter it starts increasing, which is due to change in failure and ultimate deviatoric stress with the addition of rubber. Brittleness index also decreases with the increase in confining pressure.

The results demonstrated that the rubber size tended to be more effective in increasing the shear properties of RSM. Shear strength increases with increase in rubber size up to rubber size F, but for larger rubber size G, shear strength was found lower than that for rubber size F. Considering all the rubber sizes, rubber size F provides comparatively higher shear strength, energy absorption capacity, and lower brittleness index. Hence rubber size F is considered as optimum size.

Stress-Strain plot for 30%, 50% and 75% rubber by volume in RSM compared with sand for confining pressure of 100 kPa is shown in Fig. 9. The peak and ultimate deviatoric stress of 50% RSM are higher than sand, but for 75% rubber content, the peak and ultimate deviatoric stress were close to that of sand, but with higher axial strain values for RSM. The energy absorption capacity of sand, 50% of RSM and 75% of RSM with varying confining pressure are shown in Fig. 10. Previous studies on RSM with higher rubber content suggested higher damping value and lower stiffness with high compressibility, which leads to higher settlement levels (Pitilakis et al., 2015; Zornberg et al., 2004). This compressible nature of RSM may be unfavourable for carrying gravity loads compared to conventional soil fill. In order to enhance the load carrying capacity and reduce the compressibility behaviour of RSM, reinforcement studies were carried out for the selected rubber size of F.

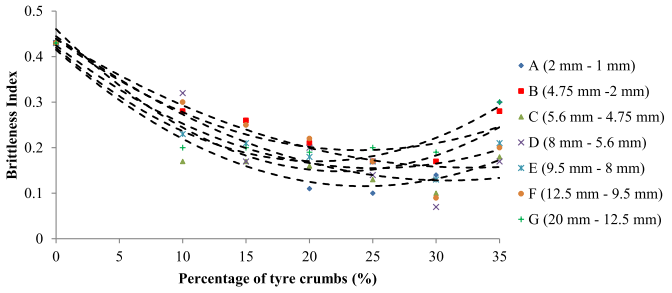

Fig. 8. Typical plot of brittleness index for different rubber sizes and contents for confining pressure of 100 kPa.

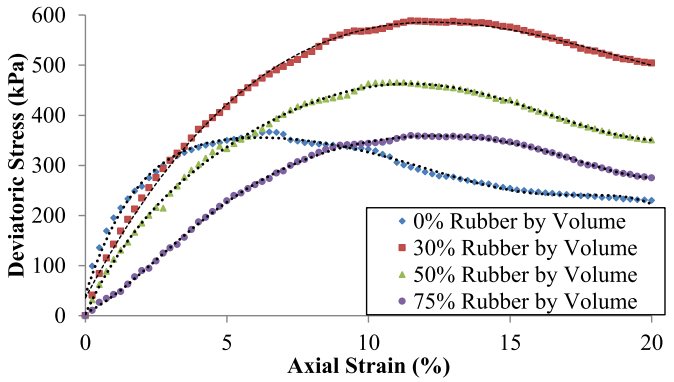

Fig. 9. Stress-Strain plot for unreinforced RSM for rubber size F at confining pressure of 100 kPa.

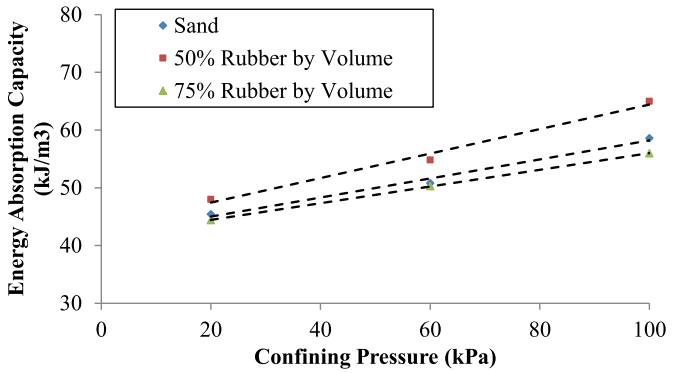

Fig. 10. Energy absorption capacity of sand and RSM.

6.2. *Stress-strain behaviour of geosynthetic reinforcement*

Reinforcement studies on RSM were carried out by considering three types of geosynthetics (i.e., geogrid, geonet and geotextile). Figs. 11 and 12 shows the comparative performance of different types of geosynthetics used in layer form (4 – layers of reinforcement, and geosynthetics arranged in 4a type, refer Fig. 4) at a confining pressure of 100 kPa for 50% and 75% RSM respectively. The stress-strain response of the unreinforced RSM is also shown in Figs. 11 and 12 for comparison. It is evident that the improvement in strength in RSM is due to reinforcing layers, and the type of reinforcement used in this study. It can be observed from the stress-strain plots, that all the reinforced RSM samples, irrespective of the kind of geosynthetic, exhibit improved response in terms of increase in peak and ultimate stresses with the corresponding

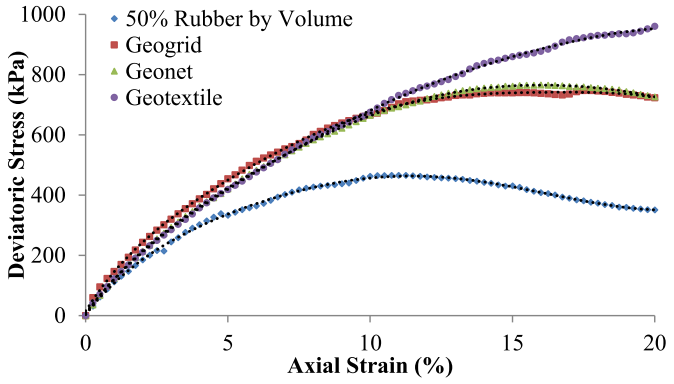

Fig. 11. Stress-Strain curve for different types of reinforcement for 50% RSM with confining pressure of 100 kPa for 4-layer of reinforcement.

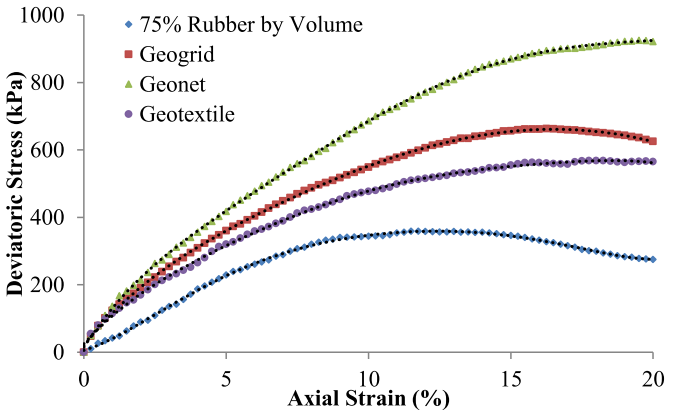

Fig. 12. Stress-Strain curve for different types of reinforcement for 75% RSM with confining pressure of 100 kPa for 4-layer of reinforcement.

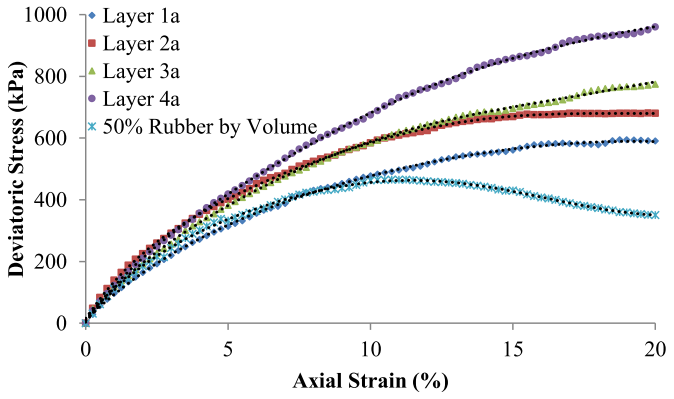

Fig. 13. Stress-Strain curve for different layering of geotextile for 50% RSM with confining pressure of 100 kPa.

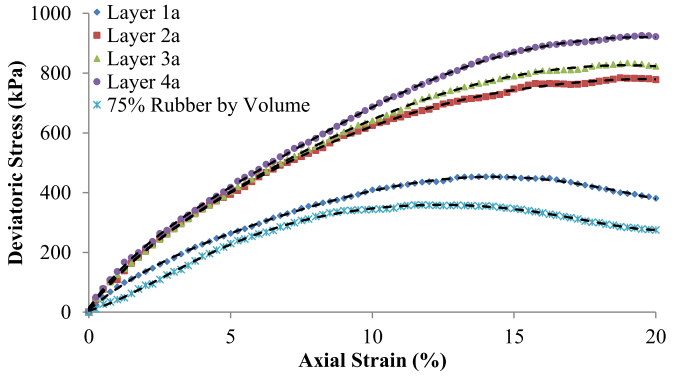

Fig. 14. Stress-Strain curve for different layering of geonet for 75% RSM with confining pressure of 100 kPa.

increase in strains. Also, the type of geosynthetic reinforcement significantly influences the peak and failure strength. The strength achieved through different forms of geosynthetic reinforcement in RSM is for an equal amount of reinforcement (the diameter of geosynthetics is kept constant). It can be observed from Fig. 11, geotextile reinforced with 50% RSM exhibits the maximum increase in shear strength for 4-layers reinforcement (arranged in 4a type) compared to geonet and geogrid reinforced RSM. The tensile strength of geotextile is 9.50 kN/m^2, which is comparatively greater than geogrid and geonet, thus geotextile exhibits higher strength for 50% RSM. Even though geogrid is with lower tensile strength values, it gives comparable results with geonet due to its similar effective opening size with rubber for 50% RSM. For 75% RSM geonet exhibits higher shear strength for 4-layer reinforcement (arranged in 4a type) compared to geogrid and geotextile (refer Fig. 12). Even though the tensile strength of geogrid is lower, but it predicts higher shear strength than geotextile in case of 75% RSM. It might be due to the lesser effective opening size (1.00 mm) of geotextile where it won't allow sand particles to move from one layer to another layer within reinforced sample creating weaker zone at the interface for higher rubber content (i.e., 75% rubber by volume) when compared to 50% RSM. Sand and RSM failed along classic shear plane close to that predicted by soil mechanics, whereas in the case of RSM reinforced with layers of geosynthetics, sample failed by bulging between two adjacent layers of reinforcement. All the reinforced RSM samples, irrespective of the kind of geosynthetic, exhibit the same failure pattern.

The geotextile aperture size and the mean size of rubber in RSM, also appear to play an important role in improving strength characteristics. More studies are required to understand the behaviour of geosynthetic aperture size and mean size of rubber in RSM's on strength characteristics of geosynthetic-reinforced RSM. It can also be noticed that the reinforced RSM exhibited higher axial strain at failure compared to that of unreinforced RSM for both 50% and 75% rubber by volume, which depends on the type of reinforcement as explained above and the number of reinforcement layers.

6.2.1. *Effect of reinforcement layer*

One of the main objectives of the present study is to observe the influence of effect of the reinforcement layer on the mechanical behaviour of reinforced RSM. For this part of the study geosynthetics which placed at equal spacing ratio (spacing between geosynthetic layers to the specimen diameter), i.e. 1a, 2a, 3a and 4a arrangement type are considered, as shown in Fig. 4. Typical stress-strain plots were given for 50% and 75% RSM reinforced by geotextile and geonet (Fig. 13 and Fig. 14) with the number of layers, as they give higher shear strength compared to other types of geosynthetics which is used as reinforcement. The effect of reinforcement clearly increases with the number of geosynthetics layer. It is evident from Figs. 13 and 14 that the shear strength of RSM increases by more than two times, for 50% RSM reinforced with 4-layer of geotextile, and 75% RSM reinforced with 4-layer of geonets compared to other geosynthetic layers (1, 2 and 3 layers). The results also demonstrated that with the increase in the layer of reinforcement, the reinforced sample exhibits a significant failure and ultimate stresses with the increase in corresponding axial strain at failure compared to unreinforced samples. With the increase in the layer of reinforcement, post-peak loss of strength was reduced. In fact, increasing the number of geotextile layers resulted in more ductility of the samples as clogging developed in the shear band within the specimens. Also, with the increase in the layer of reinforcement post-peak loss of strength was not observed (Haeri et al., 2000). The effect of layer reinforcement on strength characteristics of RSM increases with increase in confining pressure. Stiffness also increases with an increase in the type of reinforcement, the layer of reinforcement and confining pressure.

6.2.2. *Geosynthetics arrangement*

A typical plot of a stress-strain curve for different layers of geosynthetics arrangement for 50% and 75% RSM under confining pressure of 100 kPa are shown in Figs. 15 and 16. As it can be clearly noted from Figs. 15 and 16, geosynthetics arrangement in RSM has an essential role in resulting higher shear strength. The results indicated that for 50% RSM reinforced with geotextile arranged with equal spacing ratio (spacing between geotextile layers to the specimen height remains same i.e. 1a, 2a, 3a and 4a arrangement type in Fig. 4) provides higher strength than unequal spacing ratio (spacing between geotextile layers to the specimen height varies between layers i.e. 2b, 3b and 4b). It means that a single layer of geotextile in the center of the reinforced RSM specimen has almost the same effect as that of geotextile

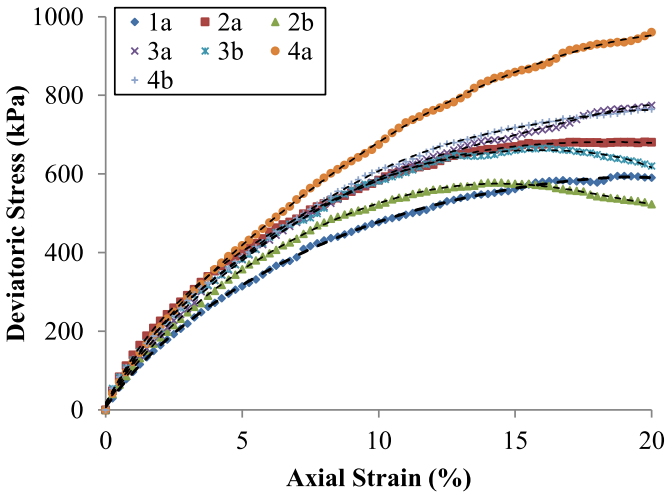

Fig. 15. Typical plot of stress-strain curve for different arrangements of geotextile layers for 50% RSM reinforced with geotextile under confining pressure of 100 kPa.

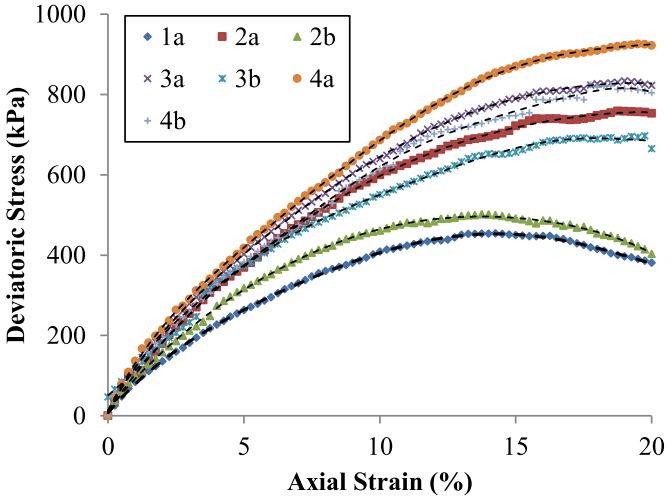

Fig. 16. Typical plot of stress-strain curve for different arrangements of geosynthetics layers for 75% RSM reinforced with geonet under confining pressure of 100 kPa.

arrangement like 2b. Similarly, two layers of geotextile arrangement in 2a type has the approximately same effect as that of three geotextile layers with an arrangement like 3b, and three layers of geotextile arrangement in 3a has the same effect as with an arrangement like 4b. Geonet arranged with equal spacing ratio provides higher shear strength than the unequal spacing ratio for 75% RSM reinforced with geonet. For 75% RSM reinforced with geonet, placed at the center has almost the same effect as geonet arrangement like 2b. Approximately, 2a type of arrangement has the same effect with an arrangement like 3b. Similarly, three layers of geonet arrangement in 3a have the same effect as with an arrangement like 4b. The reason for equal spacing ratio reinforcement predicting higher shear strength compared to the unequal spacing ratio is that most of the tensile strain occurs in the center part of the specimen compared to that of the top or bottom parts of the samples. Therefore, more tensile stresses develop in a geotextile that is placed in the middle part than other parts, and a higher strength will be reached. A single layer of geotextile in the center part of the specimen has a greater influence on the strength compared to that of a specimen with 2b arrangement. This observation (i.e. the equal spacing ratio arrangement provides maximum shear strength) can be generalized for other types of geosynthetics which are used as reinforcement for both 50% and 75% RSM.

6.2.3. *Failure and ultimate strength*

In addition of reinforcement to RSM, the stress-strain response of the RSM exhibit increase in deviatoric stress, which in turn, increase the value of failure and ultimate stresses with the corresponding increase in their axial strain. Fig. 17 shows the typical plot of deviatoric stress at failure for 50% RSM reinforced with different types of geosynthetics for 4 layers of reinforcement which are arranged in 4a type for different confining pressure. As expected from the tensile test, it can be noticed from Fig. 17, that the maximum strength is obtained for geotextile reinforcement compared to other types of reinforcement. But, geonet provides slightly higher strength compared to geogrid due to its higher tensile strength. The effect of confining pressure is clearly indicated in the strength envelops, as shown in Fig. 17. The increase in stress-strain characteristics of RSM due to the inclusion of geosynthetics, resulted in the sample being more ductile. The measure of this behaviour is given by the energy absorption capacity and brittleness index.

6.2.4. *Energy absorption capacity of reinforced RSM*

Stress-strain curve obtained from UU test for different confining pressure has been used to estimate energy absorption capacity by measuring the area under the stress-strain curve up to a strain level of 20%. A typical plot of energy absorption capacity for 50% and 75% RSM for different form and layer of reinforcement (arranged in the equal spacing ratio) at confining pressure of 100 kPa is shown in Fig. 18. In Fig. 18, the solid symbol indicates the energy absorption capacity of 50% RSM for different form and layer of reinforcement, and a hollow symbol indicates the energy absorption capacity of 75% RSM. It is shown that energy absorption capacity increases with an increasing number of layers of reinforcement for all types of geosynthetic reinforcement which is due to an increase in peak and ultimate stresses. The same trend could be observed for all confining pressure, and the energy absorption capacity increases with an increase in confining pressure. For 50% RSM, geotextile led to the highest increase in the energy absorption capacity compared to other types of geosynthetics. Similarly, for 75% RSM geonet led to the highest increase in energy absorption capacity. The energy absorption capacity increases by more than two times, for 50% RSM reinforced with 4-layers of geotextile, and 75% RSM reinforced with 4-layers of geonets.

6.2.5. *Ductility of reinforced RSM*

A typical plot of brittleness index of 75% RSM reinforced with

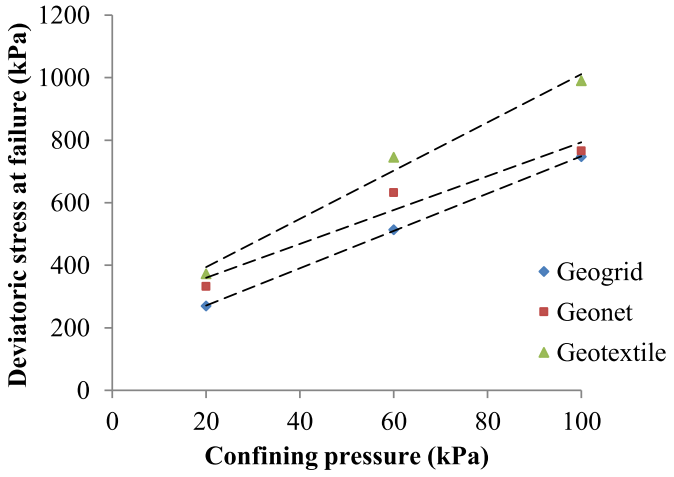

Fig. 17. Typical plot of deviatoric stress at failure for different types of geosynthetics with varying confining pressure for 50% RSM reinforced by 4a layer of reinforcement.

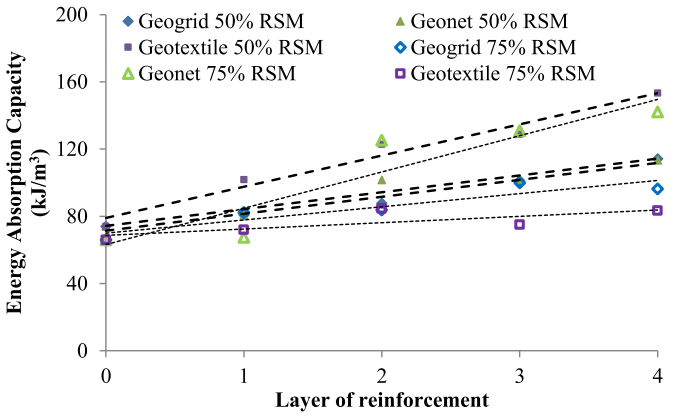

Fig. 18. Energy absorption capacity of 50% and 75% RSM for different form and layer of reinforcement (equal spacing ratio), at confining pressure of 100 kPa.

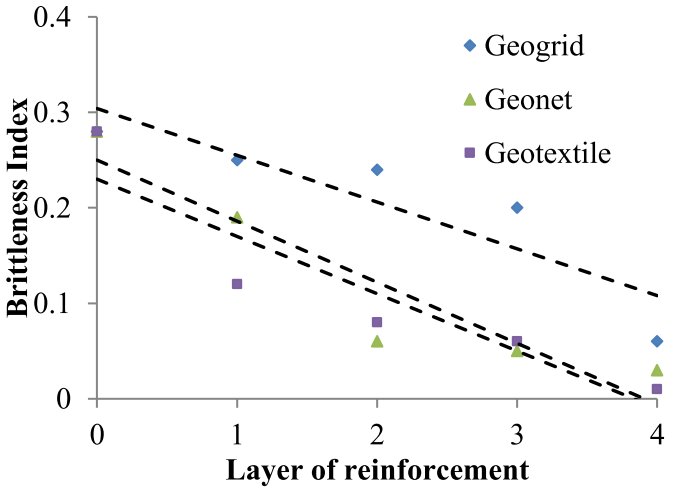

Fig. 19. Brittleness index of 75% RSM reinforced with different forms and layers (equal space ratio) for confining pressure of 100 kPa.

different forms of geosynthetics and layer (equal space ratio) of reinforcement is shown in Fig. 19. The brittleness index is a function of failure and ultimate deviatoric stress. When peak deviatoric stress is not reached in a few tests, stress corresponding to 20% strain is considered as peak and ultimate deviatoric stress to determine brittleness index. The effect of types of geosynthetics on failure and ultimate stress characteristics of RSM (50% and 75% rubber by volume) was clearly explained in earlier sections. For 50% RSM, geotextile led to higher deviatoric stress at failure and ultimate deviatoric stress compared to geonet and geogrid, which directly influence the brittleness index. For 50% RSM, geotextile inclusion reduced the brittleness index values close to zero. Geonet led to having higher deviatoric stress at failure and ultimate deviatoric stress compared to geotextile and geogrid for 75% RSM. Thus for 75% RSM, geonet have the lower brittleness index compared to other forms of geosynthetics considered in this study. For 75% RSM reinforced with geogrid tends to have different brittleness index value compared to geonet and geotextile, which might be due to lower tensile strength of geogrid. Even though for four layers of reinforcement, geogrid shows better stress-strain characteristics than geotextile (the mechanism is explained in an earlier section), but for other layers (layer 1, 2 and 3) the failure and ultimate deviatoric stress of geogrid tend to be equal or lower than geotextile and geonet.

In fact, increasing the number of geosynthetic layers resulted in less brittleness index value, which results in more ductility. Brittleness index values as low as 0.01 are noted in the above cases. The stiffness of the geosynthetic reinforced RSM increases when compared to unreinforced RSM. Stiffness also increases with an increase in the layers of reinforcement and confining pressure. With the effects of reinforcement on RSM, it becomes more capable and reliable for carrying gravity loads, and it also becomes more ductile for vibration isolation. In this investigation, all the conclusions drawn about RSM reinforced with geogrid, geonet and geotextile are limited to the chosen size, effective opening and type of reinforcement material. Further to comment about shear stiffness of reinforced RSM, numerical analysis needs to be carried out.

Reinforcement of RSM with geosynthetics will have many potential advantages for RSM in earthwork applications. Geosynthetic RSM can be used as fill materials, results in the reduction of earth pressure, reduces the deformation of facing and reduces the contact pressure with the underlying soil. Another major application of RSM is to use them as isolation material, which is discussed in the previous section. The role of rubber content in RSM on the isolation system is thoroughly studied, with shaking levels can be reduced by 60%. However, high compressibility of RSM constitutes a disadvantage, which can be overcome by the use of reinforcement. Full-scale field experiments or demonstrations are required to further validate the use of geosynthetic reinforced RSM considering the size of the specimen, boundary effect and confinement due to presence of geosynthetics in this study.

7. Summary and conclusions

This study presented the shear strength characteristics and energy absorption capacity of geosynthetic-reinforced RSM by conducting UU triaxial test. In the first part, a series of UU triaxial tests have been carried out to know the effect of rubber size on shear strength characteristics of RSM from seven different rubber sizes (A to G). RSM sample that provides higher shear strength, energy absorption capacity and stiffness is considered as the optimal size and has been used in the investigation on geosynthetic-reinforced RSM (rubber size F, passing 12.5 mm and retained on 9.5 mm sieve). The numerical studies suggest that, with the increase in rubber content in RSM, higher will be its effectiveness as vibration isolation material. To account for this, the second part of this study was carried out to investigate the shear strength and energy absorption capacity of geosynthetic-reinforced RSM by varying proportions of rubber (50% and 75% rubber by volume), type of geosynthetic (geotextile, geogrid and geonets), number of geosynthetics layers (1–4 layers), geosynthetic arrangement and confining pressure. From the geosynthetic reinforced study, the following conclusions can be drawn:

1. All reinforced RSM demonstrated significantly different stress-strain relationship as compared to unreinforced RSM. The reinforcement in RSM enhances the peak and ultimate stresses at a large axial strain.
2. Strength improvement is significantly affected by the type of geosynthetic (geogrid, geonet and geotextile) reinforcement, the number of reinforcement layers (1–4) and confining pressure.
3. RSM reinforced with geosynthetic arranged with equal spacing ratio (spacing between geotextile layers to the specimen height remains same) provides higher strength than unequal spacing ratio (spacing between geotextile layers to the specimen height varies between layers).
4. A decrease in reinforcement spacing by an increase in the number of layers of reinforcement (1–4 layers) resulted in strength improvement in reinforced RSM.
5. Fifty percent of RSM reinforced by geotextile and 75% RSM reinforced with geonets demonstrated the maximum increase in shear strength.
6. Geosynthetic reinforcement increased the energy absorption capacity by 2 times for both RSM's and reduced the brittleness index values as close to zero when compared to unreinforced RSM.

Shear strength characteristics and energy absorption capacity of geosynthetic reinforced RSM plays a very important role in the application of seismic isolation as they improve the load carrying capacity along with the corresponding increase in ductility. Energy absorption capacity calculated through static tests gives a rough estimation to select better geosynthetic reinforcement type, to select the number of layers of reinforcement, and better geosynthetic arrangement to increase the shear strength. Further, the applicability of this study can be validated through laboratory model tests and numerical simulations to determine compressible characteristics of RSM, to use them effectively in the design of reinforced RSM. From this study, the set of optimum composition of reinforced RSM was identified for estimating dynamic properties. These results can be further used to propose a promising low-cost seismic isolation method for low to moderate height building.

Acknowledgement

The authors thank, Department of Science and Technology (DST), MINISTRY OF SCIENCE & TECHNOLOGY, INDIA for funding the project titled “Low Cost Damping Materials Using Waste Tyres for Damping Isolation”, Ref: ET-004/2010 under FAST TRACK SCHEME FOR YOUNG SCIENTISTS.

References

Anastasiadis, A., Senetakis, K., Pitilakis, K., 2012. Small-Strain shear modulus and damping ratio of sand-rubber and gravel-rubber mixtures. Geotech. Geol. Eng. 30 (2), 363–382.

Anbazhagan, P., Manohar, D.R., 2015. Energy absorption capacity and shear strength characteristics of waste tire crumbs and sand mixtures. Int. J. Geotech. Earthq. Eng. 6 (1), 30–51.

Anbazhagan, P., Manohar, D.R., Rohit, Divyesh, 2015. Low cost damping scheme for low to medium rise buildings using rubber-soil mixtures. Japanese Geotechnical Society Special Publication 3 (2), 24–28.

Anbazhagan, P., Manohar, D.R., Divyesh, R., 2017. Influence of size of granulated rubber and tyre chips on the shear strength characteristics of sand-rubber mix. Geomechanics Geoengin. 12 (4), 266–278.

ASTM, 2003. Standard Practice for Classification of Soils for Engineering Purposes. Unified Soil Classification System. ASTM D2487.

ASTM, 2007a. Standard Test Methods for Density, Relative Density and Absorption of Fine Aggregate. ASTM C128.

ASTM, 2007b. Standard Test Methods for Unconsolidated Undrained Triaxial Compression Test. ASTM D2850.

ASTM, 2008. Standard Practise for Use of Scrap Tires in Civil Engineering Applications. ASTM D6270.

ASTM, 2010. Standard Test Methods for Specific Gravity of Soils by Water Pycnometer. ASTM D854.

ASTM, 2011. Standard Test Method for Determining Tensile Properties of Geogrids by the Single or Multi-Rib Tensile Method. ASTM D6637.

Backmann, H., Ammann, W., 1987. Vibrations in structures (induced by man and machines). In: Int. Assoc. For Bridge and Structural Engineering, vol. 69. IABSE – AIPC – IVBH, Zurich.

Benson, C., Olson, M., Bergstrom, W., 1996. Temperatures of an Insulated Landfill Liner. Transportation Research Record, vol. 1534 (Transportation research board, Washington, D.C).

Bergado, D.T., Tanchaisawat, T., Voottipruex, P., Kanjananak, T., 2008. Reinforced lightweight tire chips-sand mixtures for bridge approach utilization. In: Proceedings of the International Workshop on Scrap Tire Derived Geomaterials - Opportunities and Challenges - Hazarika and Yasuhara. ©2008 Taylor and Francis Group, London, pp. 151–160.

Bosscher, P.J., Edil, T.B., Kuraoka, S., 1997. Design of highway embankments using tire chips. J. Geotech. Geoenviron. Eng. 123 (4), 295–304.

Chawla, S., Shahu, J.T., Gupta, R.K., 2019. Design methodology for reinforced railway tracks based on threshold stress approach. Geosynth. Int. 26 (2), 111–120.

Correia, N.S., Zornberg, J.G., 2018. Straining distribution along geogrid-reinforced asphalt overlays under traffic loading. Geitextil and Geomembranes 46 (1), 111–120.

Dash, S.K., Choudhary, A.K., 2018. Geocell reinforcement for performance improvement of vertical plate anchors in sand. Geotext. Geomembranes 46 (2), 214–225.

Dehkordi, P.F., Ghazavi, M., Ganjian, N., Karim, U.F.A., 2019. Effect of geocell-reinforced sand base on bearing capacity of twin circular footings. Geosynth. Int. 26 (3), 224–236.

Duan, Junyi, Yang, Guolin, Lin, Yuliang, Cheng, Xinting, Dai, Zhihao, 2021. Experimental investigation of a reinforced soil retaining wall with a flexible geogrid-wrapped ecological bag facing. Geotext. Geomembranes 49, 19–31.

Edil, T.B., Bosscher, P.J., 1994. Engineering properties of tire chips and soil mixtures. Geotech. Test J. 17, 453–464, 04.

Edincliler, A., 2008. Using waste tire-soil mixtures for embankment constructions. In: Proceedings of the International Workshop on Scrap Tire Derived Geomaterials -Opportunities and Challenges- Hazarika and Yasuhara. ©2008 Taylor and Francis Group, London, pp. 319–328.

Edincliler, A., Baykal, G., Saygili, A., 2010. Influence of different processing techniques on the mechanical properties of used tires in embankment construction. Waste Manag. 30, 1073–1080.

Fei, Song, Jin, Yangtao, Liu, Huabei, Liu, Jie, 2020. Analyzing the deformation and failure of geosynthetic-encased granular soil in the triaxial stress condition. Geotext. Geomembranes 48, 886–896.

Ganeriwala, S.N., 1995. The International Society for Optical Engineering, Smart Structures and Materials, vol. 2445. Passive damping, San Diego, p. 99.

Ghadr, Soheil, Alireza, S., Bahadori, Hadi, Arya, A.L., 2020. Liquefaction resistance of fibre-reinforced silty sands under cyclic loading. Geotext. Geomembranes 48, 812–827.

Ghotbi Siabila, S.M.A., Moghaddas Tafreshia, S.N., Dawson, A.R., 2020. Response of pavement foundations incorporating both geocells and expanded polystyrene geofoam. Geotext. Geomembranes 48 (1), 1–23.

Haeri, S.M., Noorzad, R., Oskoorouchi, A.M., 2000. Effect of geotextile reinforcement on the mechanical behavior of sand. Geotext. Geomembranes 18, 385–402.

Han, B., Ling, J., Shu, X., Song, W., Boudreau, R.L., Hu, W., Huang, B., 2019. Quantifying the effects of geogrid reinforcement in unbound granular base. Geotext. Geomembranes 47 (3), 369–376.

Hayakawa, K., Nakaya, I., Asahiro, M., Kashimoto, T., Moriwaki, M., Koseki, H., 2008. In-site experiments about isolation method of ground vibration using pressed scrap tire. In: Proceedings of the International Workshop on Scrap Tire Derived Geomaterials - Opportunities and Challenges - Hazarika and Yasuhara. ©2008 Taylor and Francis Group, London, pp. 215–222.

Hazarika, H., 2008. Structural stability and flexibility during earthquakes using tyres (SAFETY) – a novel application for seismic disaster mitigation. In: Proceedings of the International Workshop on Scrap Tire Derived Geomaterials - Opportunities and Challenges - Hazarika and Yasuhara. ©2008 Taylor and Francis Group, London, pp. 115–125.

Hazarika, H., Yasuhara, K., Karmokar, A.K., Mitarai, Y., 2008a. Shake table test on liquefaction prevention using tire chips and sand mixture. In: Proceedings of the International Workshop on Scrap Tire Derived Geomaterials - Opportunities and Challenges - Hazarika and Yasuhara. ©2008 Taylor and Francis Group, London, pp. 215–222.

Hazarika, H., Kohama, E., Sugano, T., 2008b. Underwater shake table tests on waterfront structures protected with tire chips cushion. J. Geotech. Geoenviron. Eng. 134, 12.

Humphery, D.N., 2008. Tire derived aggregate as light weight fill for embankments and retaining walls. In: Proceedings of the International Workshop on Scrap Tire Derived Geomaterials - Opportunities and Challenges - Hazarika and Yasuhara. ©2008 Taylor and Francis Group, London, pp. 59–81.

Javad, Sadeghi, Ali Reza, T.K., Hossein, G., Mosarreza, F.M., Sepehr, M., 2020. Effectiveness of geogrid reinforcement in improvement of mechanical behaviour of sand-contaminated ballast. Geotext. Geomembranes 48, 768–779.

Kaneko, T., Orense, R., Hyodo, M., Yoshimoto, N., 2013. Seismic response characteristics of saturated sand deposits mixed with tire chips. Geotechnical and Geoenvironmental Engineering 139 (4), 633–643.

Kirzhner, F., Rosenhouse, G., Zimmels, Y., 2006. Attenuation of noise and vibration caused by underground trains, using soil replacement. Tunn. Undergr. Space Technol. 21, 561–567.

Lee, J.H., Salgado, R., Bernal, A., Lovell, C.W., 1999. Shredded tires and rubber-sand as lightweight backfill. Geotechnical and Geoenvironmental Engineering 125, 2.

Liang, Lu, Shuwen, Ma, Wang, Zongjian, Zhang, Yi, 2021. Experimental study of the performance of geosynthetic-reinforced soil walls under differential settlements. Geotext. Geomembranes 49, 97–108.

Masad, E., Taha, R., Ho, C., Papagiannakis, T., 1996. Engineering properties of Tire/Soil mixtures as a lightweight fill material. Geotech. Test J. 19 (3), 297–304.

Mehrjardi, G.T., Behrad, R., Tafreshi, S.N.M., 2019. Scale effect on the behaviour of geocell-reinforced soil. Geotext. Geomembranes 47 (2), 154–163.

Moghaddas Tafreshi, S.N., Norouzi, A.H., 2012. Bearing capacity of square model footing on sand reinforced with shredded tire-An experimental investigation. Construct. Build. Mater. 35, 547–556.

Mousavi, S., Gabr, M.A., Borden, R.H., 2017. Optimum location of geogrid reinforcement in unpaved road. Can. Geotech. J. 54 (7), 1047–1054.

Muhammad Nouman, A.R., Sanjay Kumar, S., 2020. Ultimate bearing capacity of strip footing resting on soil bed strengthened by wraparound geosynthetic reinforcement technique. Geotext. Geomembranes 48, 867–874.

Pitilakis, A., Karapetrou, S., Tsagdi, K., 2015. Numerical investigation of the seismic response of RC buildings on soil replaced with rubber-sand mixtures. Soil Dynam. Earthq. Eng. 79, 237–252.

Roylance, D., 2001. Stress-Strain Curves. Department of Materials Science and Engineering, Massachusetts Institute of Technology, Cambridge.

Santiago, B., Jaun Carlos, L., Eduardo, K., 2016. Non-linear modelling of seismic isolation systems made of recycled tire-rubber. Soil Dynam. Earthq. Eng. 85, 134–145.

Satyal, S.R., Leshchinsky, B., Han, J., Neupane, M., 2018. Use of cellular confinement for improved railway performance on soft subgrades. Geotextile and geomembranes 46 (2), 190–205.

Selcuk, Bildik, Mustafa, Laman, 2020. Effect of geogrid reinforcement on soil structure pipe interaction in terms of bearing capacity, settlement and stress distribution. Geotext. Geomembranes 48, 844–853.

Senetakis, K., Anastasiadis, A., Pitilakis, K., 2012. Dynamic properties of dry sand/rubber (SRM) and gravel/rubber (GRM) mixtures in a wide range of shearing strain amplitudes. Soil Dynam. Earthq. Eng. 33, 38–53.

Shadmand, A., Ghazavi, M., ganjian, N., 2018. Load-settlement characteristics of large-scale square footing on sand reinforced with opening geocell reinforcement. Geotextile and geomembranes 46 (3), 219–226.
Sheikh, M., Mashiri, M.H., Vinod, J.S., Tsang, Hing-Ho, 2013. Shear and compressibility behaviours of Sand-Tyre Crumb mixtures. J. Mater. Civ. Eng. 25 (10), 1366–1374.
Song, F., Liu, H.B., Xie, Y.L., 2018. Centrifuge tests of geocell-reinforced retaining walls at limit equilibirium. J. Geotech. Geoenviron. Eng. 144 (3), 04018005.
Tafreshi, S.N.M., Rahimi, M., Dawson, A.R., Leshchinsky, B., 2019. Cyclic and post-cycling anchor response in geocell-reinforced sand. Can. Geotech. J. 56 (11), 1700–1718.
Tafreshi, S.N.M., Darabi, N.J., Dawson, A.R., 2020. Combining EPS geofoam with geocell to reduce buried pipe loads and trench surface rutting. Geotext. Geomembranes 48 (3), 400–418.
Tatlisoz, N., Edil, T.B., Benson, C.H., 1998. Interaction between reinforcing geosynthetics and soil-tire chip mixtures. J. Geotech. Geoenviron. Eng. 124, 11.
Tsang, H.H., 2008. Seismic isolation by rubber-soil mixtures for developing countries. Earthq. Eng. Struct. Dynam. 37 (2), 283–303.
Tsang, H.H., 2009. Geotechnical Seismic Isolation. Earthquake Engineering: New Research. Nova Science Publishers Inc, New York, USA, pp. 55–87.
Tsang, H.H., Lo, S.H., Xu, X., Sheikh, M.N., 2012. Seismic isolation for low-to-medium-rise buildings using granulated rubber-soil mixtures: numerical study. Earthq. Eng. Struct. Dynam. https://doi.org/10.1002/eqe.2171.
Venkateswarlu, H., Ujjwal, K.N., Hegde, A., 2018. Laboratory and numerical investigation of machine foundations reinforced with geogrids and geocells. Geotext. Geomembranes 46 (6), 882–896.
Wang, J.Q., Zhang, L.L., Xue, J.F., Tang, Y., 2018. Load settlement response of shallow square footing on geogrid-reinforced sand under cyclic loading. Geotext. Geomembranes 46 (5), 586–596.
Xiong, W., Yan, M., Li, Y., 2014. Geotechnical seismic isolation system further experimental study. Appl. Mech. Mater. 580–583, 1490–1493.
Yegian, M.K., Catan, M., 2004. Soil isolation for seismic protection using a smooth synthetic liner. J. Geotech. Geoenviron. Eng. 130 (11), 1131–1139.
Yegian, M.K., Kadakal, U., 2004. Foundation isolation for seismic protection using a smooth synthetic liner. J. Geotech. Geoenviron. Eng. 130 (11), 1121–1130.
Yoon, Y.W., 2008. Engineering characteristics of tire treads for soil reinforcement. In: Proceedings of the International Workshop on Scrap Tire Derived Geomaterials - Opportunities and Challenges - Hazarika and Yasuhara. ©2008 Taylor and Francis Group, London, pp. 83–105.
Yoon, Y.W., Heo, S.B., Kim, K.S., 2008. Geotechnical performance of waste tires for soil reinforcement from chamber tests. Geotext. Geomembranes 26 (1), 100–107.
Zornberg, J., Cabral, A., Viratjandr, C., 2004. Behaviour of tire shred sand mixtures. Can. Geotech. J. 41, 227–241.